Midinfrared spectrum of undoped cuprates

Graaf, de, Coen; Broer, Ria

Published in:
Physical Review B

DOI:
10.1103/PhysRevB.62.702

Publication date:
2000

Midinfrared spectrum of undoped cuprates: *d-d* transitions studied by *ab initio* methods

Coen de Graaf*
Departament de Química Física i Centre de Recerca en Química Teòrica, Universitat de Barcelona, C/Martí i Franquès 1, 08028 Barcelona, Spain

Ria Broer
Theoretical Chemistry, Materials Science Center, University of Groningen, Nijenborgh 4, 9747 AG Groningen, The Netherlands
(Received 30 November 1999)

We present results of *ab initio* calculations for *d-d* transitions, which arise in the midinfrared spectrum of undoped cuprate compounds. It has been suggested that these transitions arise at energies as low as 0.4 eV in La_2CuO_4 and $Sr_2CuO_2Cl_2$. We study the differences in *d-d* transition energies in a series of cuprates that contains compounds in which the Cu ions are sixfold, fivefold, or fourfold coordinated. Furthermore, we analyze the dependence of the $3d_{x^2-y^2} \rightarrow 3d_{z^2}$ excitation energy on the ratio of the in-plane and apex copper—ligand distances in the model system CuO. Our cluster calculations do not support the assignment of the 0.4–1-eV band to phonon and magnon sidebands of a *d-d* transition. On the other hand, we confirm the interpretation of the peak around 1.7 eV observed in $CuGeO_3$ as arising from *d-d* transitions.

I. INTRODUCTION

The undoped parent compounds of the lamellar cuprate superconductors are classified as so-called charge-transfer (CT) insulators with a band gap of about 2 eV. Recent experiments have revealed a variety of optical absorptions within the band gap of these and related compounds, the origin of which is a subject of discussion. Already in the 1960s, Mizuno and Koide discussed the origin of similar peaks observed in NiO and $KNiF_3$ and attributed the absorption to a process in which two magnons and a phonon are created.[1] The phonon excitation lowers the lattice symmetry and makes the forbidden two-magnon absorption allowed. Only recently, Lorenzana and Sawatzky have proposed a theory that describes such a so-called phonon-assisted multimagnon absorption.[2,3] The theory was successfully applied to La_2NiO_4 and La_2CuO_4 to reproduce both the excitation energy and the line shape of the absorption with satisfactory accuracy. However, a problem arises for La_2CuO_4 and other cuprates. For these materials the sharp peak is measured at 0.4 eV, and a broad, rather intense, sideband is observed at higher energies, which extends up to 1.0 eV. This sideband is much weaker in La_2NiO_4. Perkins and co-workers argued that the sideband cannot be explained by phonon-assisted multimagnon absorptions in which more than two magnons are created.[4–6] Their reasoning is based on the assumption that the intensity of the phonon-assisted multimagnon absorptions increases by at most a factor of 2 comparing a $S=1$ with a $S=\frac{1}{2}$ Heisenberg antiferromagnet. This is in sharp contrast with the observed increase with a factor of 50 in the case of La_2NiO_4 and La_2CuO_4. Instead, Perkins *et al.*[6] propose to consider the possibility that the broad 0.4–1-eV bands in La_2CuO_4 are phonon and magnon sidebands of a Cu crystal field excitation at $\sim$0.5 eV. Examples are given of materials in which the latter excitations are observed with intensities comparable to La_2CuO_4. However, the explanation of Perkins *et al.* also has a serious drawback, namely, cluster calculations, both *ab initio* and semiempirical, predict the lowest *d-d* transition to appear at energies around 1.0–1.5 eV.[7,8]

In this paper, we present *ab initio* cluster calculations of the *d-d* transition energies in a series of different copper oxides, La_2CuO_4, $Sr_2CuO_2Cl_2$, $CuGeO_3$, $YBa_2Cu_3O_6$, Ca_2CuO_3, and Sr_2CuO_3. The compounds in this series show a variety of copper coordinations, ranging from square planar for the spin-$\frac{1}{2}$ chain compounds Ca_2CuO_3 and Sr_2CuO_3 to a distorted octahedral coordination for La_2CuO_4. The other three compounds are intermediate cases; in $CuGeO_3$ and $Sr_2CuO_2Cl_2$ the Cu ions also have an octahedral coordination but the apical anions (O for $CuGeO_3$ and Cl for $Sr_2CuO_2Cl_2$) lie relatively far away, 2.76 and 2.86 Å, respectively. In $YBa_2Cu_3O_6$, the Cu^{2+} ions have a fivefold coordination. Table I gives an overview of the Cu-ligand distances of the compounds considered.

In addition, we report the results obtained for La_2NiO_4 and CuO. These compounds were added for two different reasons; La_2NiO_4 because the transition energies of the *d-d* excitations are experimentally rather well resolved and CuO to further investigate the dependence of the $3d_{x^2-y^2}$ to $3d_{z^2}$

TABLE I. Overview of the Cu-ligand distances in the series of cuprates considered. In case of nonoxygen ligands, the kind of ligand is given in parentheses.

	Cu-$O_{\text{in-plane}}$ distance (Å)		Cu-L_{apex} distance (Å)	
	x	y	$+z$	$-z$
CuO	2.044	2.044	2.044	2.044
La_2CuO_4	1.905	1.905	2.397	2.397
$CuGeO_3$	1.942	1.942	2.764	2.764
$Sr_2CuO_2Cl_2$	1.986	1.986	2.859 (Cl)	2.859 (Cl)
$YBa_2Cu_3O_6$	1.942	1.942	2.466	3.282 (Cu)
Ca_2CuO_3	1.894	1.962	3.250 (Cu)	3.250 (Cu)
Sr_2CuO_3	1.954	1.960	3.494 (Cu)	3.494 (Cu)

excitation energy on the ratio of the Cu-O_{apex} and Cu-$O_{in\text{-}plane}$ distances.

The paper is organized as follows: in the next section, we briefly resume experimental data and further structural characteristics of the compounds considered. Thereafter, a description is given of the computational approach followed to obtain *ab initio* estimates of the *d-d* transition energies in the different cuprates. The next section gives an overview of all results. Attention is focused on the dependence of the different excitations energies on the structural details of the cuprate series. Final results are compared with experiment and we show that the hypothesis of Perkins *et al.* about the 0.4–1-eV band is not supported by state-of-the-art cluster calculations. Finally, we give a short summary of the most relevant conclusions.

II. EXPERIMENTAL DATA

Experimental evidence of *d-d* transitions in insulating cuprates was found in Raman-scattering experiments of Liu *et al.* and Salomon *et al.*[9,10] They observe features of A_{2g} symmetry in the 1.5–1.7-eV region in a large series of cuprates, which have been ascribed to *d-d* transitions connected to the replacement of a hole from the $3d_{x^2-y^2}$ orbital to the $3d_{xy}$ orbital (for local D_{4h} symmetry: $B_{1g}\otimes B_{2g}=A_{2g}$). For La_2CuO_4 this peak is observed at 1.70 eV, while in $YBa_2Cu_3O_6$ the peak arises at 1.54 eV. Electroreflectance experiments performed by Falck *et al.*[11] provide additional indications for the existence of *d-d* transitions in La_2CuO_4. Excitations near 1.4 and 1.6 eV have been observed, which were ascribed to final states of B_{2g} ($3d_{xy}$) and E_g ($3d_{xz,yz}$) site symmetry, respectively. More recently, Kuiper *et al.* have measured the x-ray Raman spectrum of $Sr_2CuO_2Cl_2$.[12] The transitions to the $3d_{xy}$ and $3d_{xz,yz}$ states were located at 1.35 and 1.7 eV, while the transition to the $3d_{z^2}$ state could not be directly observed. However, it is argued that this transition must be hidden under the $3d_{xz,yz}$ peak and is accompanied by a so-called spin-flip excitation of roughly 0.2 eV. Hence, the *d-d* transition energy to the $3d_{z^2}$ state was estimated to be $\sim$1.5 eV.

Several papers have reported midinfrared absorptions around 0.5 eV. Besides the work of Perkins *et al.*, such low excitations have also been observed by Grüninger *et al.* in transmission and reflection measurements on $YBa_2Cu_3O_6$.[13] By assuming a relative large interplanar magnetic coupling, the peaks observed at 0.34 and 0.46 eV could be explained by phonon-assisted magnon absorption processes. Furthermore, the absorption spectrum of Sr_2CuO_3 shows a peak centered at 0.48 eV.[14] This peak is also ascribed to a phonon-assisted bimagnon absorption and has been successfully fitted with the theory of Lorenzana and Sawatzky.[15]

The infrared absorptions in $CuGeO_3$ have been interpreted in two different ways. Terasaki *et al.*[16] observe sharp peaks at 1.25, 2.88, and 3.66 eV. The lowest absorption has been ascribed to a local CT excitation between O-2*p* and Cu-3*d* orbitals. The second peak is assumed to arise from a *d-d* transition or possibly from an interband transition. The third peak was not explicitly assigned. On the other hand, optical absorption experiments by Bassi *et al.*[17] and electron-energy-loss spectroscopy (EELS) experiments by Corradini *et al.*[18] claim a different interpretation. A first peak at 1.7 eV with onset at 1.3 eV is ascribed to *d-d* transitions, whereas a strong exponential increase in the absorption is observed starting approximately at 3 eV attributed to the onset of CT transitions.

Finally, we list the different peaks observed in the optical spectrum of La_2NiO_4.[5] Contrary to the cuprates listed above, the assignment of the peaks in the midinfrared spectrum of La_2NiO_4 is well established. First there is the multimagnon peak at 0.25 eV mentioned already. Two additional broad peaks are observed, both ascribed to *d-d* transitions. The first peak can be resolved in a mean peak at 1.05 eV and a shoulder at 1.25 eV, the second peak is interpreted as a superposition of two absorptions at 1.6 and 1.75 eV, respectively. By comparing these data to the experimental data for NiO,[19] it is observed that the values for La_2NiO_4 are similar to those for NiO. The additional splittings of the peaks are explained by the lower site symmetry in La_2NiO_4, i.e., D_{4h} instead of O_h. Based on these considerations the following assignment can be made: the peaks at 1.05 and 1.25 eV arise from transitions to the a^3E_g and a^3B_{2g} states. These states originate from the $^3T_{2g}$ state in O_h symmetry. The peaks at 1.6 and 1.75 eV can be assigned to the transitions to b^3B_{2g} and b^3E_g, originating from the $^3T_{1g}$ state, although for these peaks additional contributions from the peaks arising from the singlet state in O_h symmetry, a^1E_g, cannot be excluded beforehand.

III. STRUCTURAL INFORMATION

Although CuO does not have a rocksalt structure, we assume a simple cubic structure in which the Cu has O_h site symmetry. This is done in order to use the compound as a model system to study the dependence of the *d-d* transition energies on the ratio between the Cu-$O_{in\text{-}plane}$ and Cu-O_{apex} distances. For this purpose, we elongate the Cu-O_{apex} distance from 2.044 Å—corresponding to the Cu-O distance in the experimental monoclinic structure[20]—to 2.555 Å in four steps and calculate the transition energies at each of the five different ratios.

Without considering the small distortions in the crystal structure, La_2NiO_4, La_2CuO_4, and $Sr_2CuO_2Cl_2$ belong to the same structural family described by the space group $I4/mmm$. The structure is characterized by transition-metal (TM) O_2 planes formed by corner sharing TM O_4 squares. These planes are intermediated by a double layer containing the apex ligands (O and Cl) and the counterions (La and Sr). Figure 1 shows the idealized crystal structure of La_2NiO_4 taken from experiment.[21–23] Structural data for La_2CuO_4 is taken from Ref. 24 and for $Sr_2CuO_2Cl_2$ from Ref. 25.

The crystal structure of $CuGeO_3$ is characterized by spin-$\frac{1}{2}$ chains formed by edge sharing CuO_4 squares. These chains are connected by tetrahedrally coordinated Ge atoms; see Fig. 2. It is well known that $CuGeO_3$ undergoes a spin-Peierls transition at 14 K, however, in the calculations we use the undistorted crystal structure with space group *Pmma* as determined by Völlenkle *et al.*[26] Figure 3 illustrates the crystal structure of $YBa_2Cu_3O_6$. The Cu^{2+} ions with unpaired electrons are located in the distorted CuO_2 planes intermediated by yttrium ions. The copper ions on the corners of the unit cell have formal charge of $+1$ and hence possess a closed-shell configuration and therefore do not give rise to any *d-d* transitions. The structure has a $P4/mmm$ space

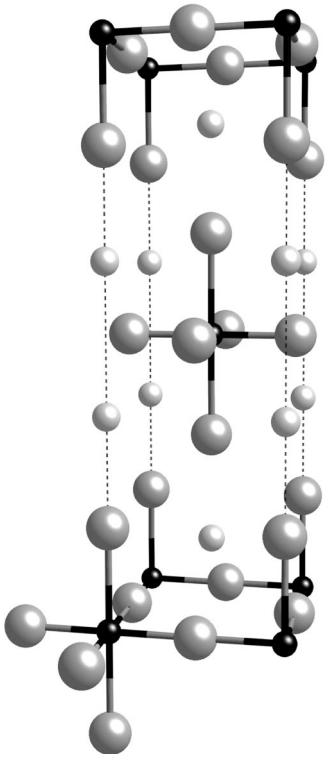

FIG. 1. Crystal structure of La_2NiO_4. Dark spheres represent Ni ions, light spheres represent oxygen (large spheres) and La (smaller spheres). The unit cell is formed by the thin lines and the thicker lines connect nickel and oxygen ions.

group and the experimental data are taken from Ref. 27.

Finally, the structure of Sr_2CuO_3 and Ca_2CuO_3 closely resembles the La_2CuO_4 structure, except for the fact that copper ions are connected by oxygens in one direction only. This gives rise to the formation of virtualy isolated spin-$\frac{1}{2}$ chains with large antiferromagnetic interaction. Therefore these compounds are considered to be the best experimental realizations of a one-dimensional (1D) spin-$\frac{1}{2}$ system. The space group for both compounds is I/mmm and the lattice parameters are taken from Ref. 28 for Ca_2CuO_3 and Ref. 29 for Sr_2CuO_3. In the calculations the coordinate axes are chosen such that the four oxygens that coordinate the copper ions lie in the x-y plane. With this choice the electron hole in the ground state has $3d_{x^2-y^2}$ character.

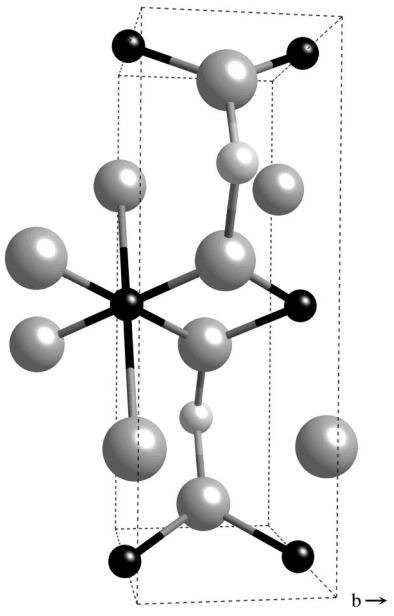

FIG. 2. Crystal structure of $CuGeO_3$. Dark spheres represent Cu ions, large light spheres O, and small light spheres Ge. Spin chains of edge sharing CuO_4 squares are formed in the b direction. For one of the Cu ions, the sixfold coordination is shown.

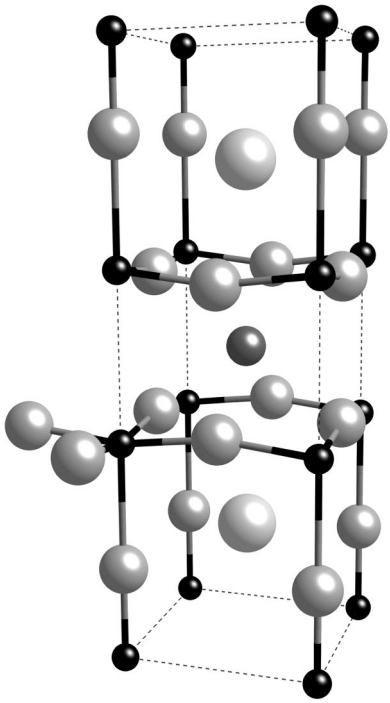

FIG. 3. Crystal structure of $YBa_2Cu_3O_6$. Small dark spheres represent Cu ions, light small spheres represent oxygen ions. The large spheres depict Y (dark) and Ba (light) ions. For one of the Cu^{2+} ions the full fivefold coordination is illustrated.

IV. COMPUTATIONAL APPROACH

The localized character of the $3d^n$ states makes the cluster model approach a natural starting point to investigate the relative energies of these states. Applications of the cluster model approach in a wide variety of systems have shown the ability of this method to calculate and predict the excitation energies of the *d-d* transitions.[8,30–35] A common choice for the cluster is to include the transition metal (TM) and the first shell of ligands (L). The electronic structure of these ions are described in a very accurate manner, whereas the effect of the rest of the crystal is included in a more approximate way by neglecting all interactions with the cluster atoms except for the electrostatic interaction.

Such TM-L_x clusters embedded in point charges only are not appropriate for most of the materials considered here. Because of the high formal ionic charge of some of the counterions (La^{3+}, Ge^{4+}, and Y^{3+}) coordinating the oxygen ions in the cluster, the cluster wave function has the tendency to delocalize towards the point charges, especially when basis sets for oxygen are used that contain rather diffuse orbitals. To avoid the spurious charge flow it is necessary to account for the Pauli repulsion between the cluster ions and these

neighboring counterions. Moreover, it has recently been found that the relative energies change by a small, although significant amount when the cluster model accounts for the Pauli repulsion between the cluster ions and the ions in the direct surrounding.[36] The simplest way is to represent the counterions by some kind of repulsive potential, however, in the present application, we include these counterions in the cluster model, hence allowing for an accurate *ab initio* treatment of the Pauli repulsion. After discussing the computational scheme to obtain accurate *N*-electron wave functions for the different $3d^n$ states, we will give more details about the explicit representation of the counterions.

Atomic natural orbital (ANO) Gaussian-type functions are used to describe the one-electron orbital space.[37–39] For the TM ions a $(21s, 15p, 10d, 6f)/[6s, 5p, 3d, 1f]$ basis set is applied, for oxygen $(14s, 9p, 4d)/[5s, 4p, 1d]$, and for chlorine $(17s, 12p, 5d)/[5s, 4p, 1d]$. To account for the important electron correlation effects present in the cuprates and La_2NiO_4, *N*-electron wave functions are constructed in two different approximations. First a complete active space self-consistent-field (CASSCF) wave function is constructed with an active space that contains 9 (Cu) or 8 (Ni) electrons and ten orbitals, i.e., the five TM-$3d$ orbitals and five virtuals with the same symmetry character, the so-called d' orbitals. Subsequently, complete active space second-order perturbation theory (CASPT2) is used to correlate the TM-$3s$, $3p$, and $3d$, and the *L-ns* and *np* (for oxygen: $2s$, $2p$, and for Cl: $3s$, $3p$) electrons. In this approximation the CASSCF wave function is taken as zeroth-order wave function and the remaining electron correlation effects are estimated by second-order perturbation theory.[40,41] All calculations are performed with MOLCAS version 4.[42]

The explicit inclusion of the counterions in Ca_2CuO_3 does not lead to serious problems. Because of the relative few number of electrons present in Ca^{2+}, these counterions can be included at an all-electron (AE) level with a reasonably large basis set (e.g., $[5s, 4p, 1d]$) without increasing the calculation to an unmanageable size. However, for all other compounds the counterions are of such size that an AE description of these ions leads to very large calculations, and moreover, relativistic corrections need to be included for the heavier ions. For these reasons the core electrons of the counterions are described with an *ab initio* model potential (AIMP) (Ref. 43) that not only largely reduces the size of the calculation but also accounts for scalar relativistic effects. The valence np^6 electrons are described with $(2s, 3p, 2d)$ basis set. The AIMP for the Ge counterions in $CuGeO_3$ includes the $[\mathrm{Ar}, 3d]$ core, leaving zero electrons to be described assuming a formal ionic charge of $4+$ for Ge. However, the $[2s, 3p, 2d]$ basis set allows the Ge ion to pick up electrons and form covalent bonds with the oxygen ions.

The validity of a description of the core electrons with model potentials is checked for Ca_2CuO_3 for which AE and model potential results can be compared. Figure 4 shows the theoretical excitation energies of the *d-d* transitions in Ca_2CuO_3 obtained with a CuO_4Ca_8 cluster embedded in point charges. The energies in the level diagram are obtained by CASPT2 as explained above. In the first column the 8 Ca ions are represented as frozen ions. The charge distribution of the frozen ions is obtained in a separate Hartree-Fock calculation on the $[Ca_8]^{16+}$ fragment with a $[3s, 2p]$ minimal basis set. Thereafter the orbitals of the CuO_4 fragment are Gramm-Schmidt orthogonalized onto the Ca_8 fragment and in the subsequent CASSCF/CASPT2 calculations the orbitals of the Ca ions are kept frozen. The next columns show the results of calculations in which the Ca ions are described with an AE basis set of triple zeta valence quality (TZV) quality. The excitation energies hardly change compared to the frozen ion description. However, when polarization functions are added to the Ca^{2+} ions, a drop in the excitation energies of about 0.2 eV is found. These lower energies are reproduced when the inner core of the Ca ions is represented with an AIMP, combined with a basis set contraction recommended in the original reference,[43] namely, $[2s, 3p, 3d]$. The reduction of the number of *d* functions to 2 does not affect the excitation energies, while a reduction of the basis set to double zeta valence (DZV) quality (levels in the last column) increases all energies by a significant amount and tend towards the frozen ion results. Hence it can be concluded that the AIMP's combined with a $[2s, 3p, 2d]$ basis set is the most appropriate choice to represent the counterions. Note that the quality of the basis set associated with the counterions is large enough to account for dynamical electron correlation effects, and hence the *np* electrons are also correlated in the CASPT2 calculation. Nevertheless, it is expected that the contribution of this effect to the relative energies is rather small. In fact, we observe a very small (<0.05 eV) difference in the effect of CASPT2.

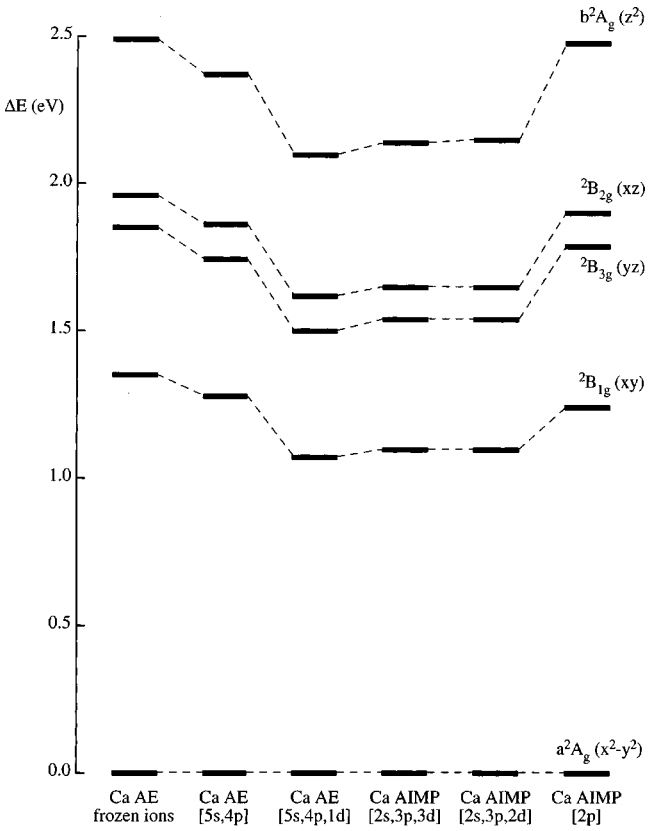

FIG. 4. CASPT2 excitation energies in eV of the *d-d* transitions in Ca_2CuO_3 for different representations of the 8 Ca^{2+} ions included in the cluster. The hole character of each state is given in parentheses.

The cluster models used in the calculations are the following: CuO_4Ca_8 and CuO_4Sr_8 for Ca_2CuO_3 and Sr_2CuO_3, re-

TABLE II. Relative energies (in eV) for the *d-d* transitions in La_2NiO_4 obtained by CASSCF and CASPT2. Energies are compared to experimental data of Perkins *et al.* (Ref. 5).

State	CASSCF	CASPT2	Expt
$^3B_{1g}$	0.00	0.00	
a^3E_g	0.78	0.89	1.05
a^3B_{2g}	1.14	1.25	1.25
b^3B_{2g}	1.54		1.60
b^3E_g	1.74	1.71	1.75
$^1A_{1g}$	1.84	1.68	
$^1B_{1g}$	2.17	1.77	
^1E_g	2.83	2.56	
$^1B_{2g}$	3.32	3.01	

TABLE III. CASPT2 energies (in eV) of the *d-d* transitions in a series of cuprates compared to available experimental data. The different $3d^9$ states are characterized by the character of the singly occupied orbital, i.e., the hole character.

	Hole character						
	x^2-y^2	z^2	xy	xz	yz	xy (expt)	xz, yz (expt)
CuO	0.00	0.00	1.02	1.02	1.02		
La_2CuO_4	0.00	0.99	1.29	1.57	1.57	1.4, 1.7	1.6
$CuGeO_3$	0.00	1.75	1.41	1.70	1.70	1.3, 2.9	1.7
$Sr_2CuO_2Cl_2$	0.00	1.18	1.23	1.50	1.50	1.4	1.7
$YBa_2Cu_3O_6$	0.00	1.69	1.21	1.61	1.61	1.5	
Ca_2CuO_3	0.00	2.15	1.10	1.65	1.54		
Sr_2CuO_3	0.00	2.11	1.08	1.67	1.53		

spectively; $CuO_5Y_4Ba_4$ for $YBa_2Cu_3O_6$; CuO_6Ge_4 for $GeCuO_3$; $CuO_4Cl_2Sr_8$ for $Sr_2CuO_2Cl_2$; and TM O_6La_{10} for La_2TMO_4 (TM=Cu, Ni). For the model system CuO a simple CuO_6 cluster is used. All clusters are embedded in either a small set of optimized point charges or a large array of point charges with the formal ionic value, always terminated by a shell of Evjen charges[44] to ensure the overall charge neutrality. The nearest-neighbor Cu ions in the CuO_2 chain in $GeCuO_3$ (see Fig. 2) and the Cu ion in the adjacent CuO_2 plane in $YBa_2Cu_3O_6$ (see Fig. 3) are included as frozen ions. To avoid that open shell orbitals have to be kept frozen (a feature, which is not implemented in our programs), the calculations are done with frozen Mg^{2+} ions. These ions have ionic radii that are virtually equal: 0.86 vs 0.87 Å in a sixfold coordination and 0.71 Å for a fourfold coordination,[45] and hence the frozen Mg^{2+} ions are expected to reproduce fairly well the Pauli repulsion of the Cu^{2+} ions.

V. RESULTS AND DISCUSSION

Because of the noncontroversial assignment of the peaks in the midinfrared spectrum of La_2NiO_4, we first apply the computational scheme explained in the previous section to calculate the *d-d* transition energies in this compound. In this way an estimate can be obtained of the accuracy of the method in reproducing the relative energies of the different $3d^n$ states. The method has been applied before to simpler structures as NiO and CoO,[33,36,46] and it was found that excitation energies are reproduced within 0.15 eV compared to experimental data. These studies also revealed that relativistic effects, both scalar and spin-orbit interaction, are relatively unimportant for the *d-d* transition energies in compounds containing first-row TM ions.

Table II lists the CASSCF and CASPT2 energies and compares them to the experimental data of Perkins *et al.*[5] The CASSCF energies already give a rather satisfactory estimate of the transition energies. The relative order of the $3d^8$ states is in agreement with the one expected from the symmetry considerations discussed above. The treatment of the remaining electron correlation by means of CASPT2 has a very similar effect on the excitation energies as observed previously for NiO, i.e., a small increase of the excitation energy for the lower *d-d* transition and a decrease for the higher-lying states. The b^3B_{2g} state is largely affected by intruder states that cause a severe breakdown of the perturbation theory. In principle, two solutions exist to this problem. The best solution is to include the intruder states in the CASSCF wave function, but in the present case this leads to an active space of unmanageable size. The other, more pragmatic, solution is to apply a level-shift technique;[47] the near degeneracies are removed by artificially shifting up in energy all external configurations by an arbitrary amount and later correcting the calculated second-order energy for the applied shift. This method works very well provided that the interaction matrix element of the intruder state with the reference wave function is small and the applied shift does not get extremely large. However, for the b^3B_{2g} state the interfering effect of the intruder states cannot be removed unless relatively large (0.4 hartree) shifts are applied and for this reason, no reliable CASPT2 excitation energy can be given. It is, however, not expected that the differential electron correlation is very different from the other states, and hence the assignment of this state to the peak observed at 1.60 eV seems very reasonable.

The CASPT2 energies confirm the assignment of the peaks observed in the absorption spectrum of La_2NiO_4. As already mentioned above, we indeed observe excitation energies in the region of 1.5–1.8 eV arising from states that originate from both the $^3T_{1g}$ and the ^1E_g state. The results for La_2NiO_4 listed in Table II clearly indicate that the present choice of the material model and approximation of the *N*-electron wave function are sufficient to obtain reasonable estimates of the excitation energies for TM materials that have a more complex structure than the simple rocksalt TM oxides. For all levels the estimated transition energies lie within the typical accuracy of about 0.15 eV of the applied method.

We now discuss the *ab initio* estimates of the *d-d* transitions in the series of cuprates introduced in Sec. I. The first compound listed in Table III is the model system CuO in a rocksalt structure. Because of the octahedral symmetry, there is only one *d-d* transition possible, namely from the ^2E_g ground state to the $^2T_{2g}$ excited state. The degeneracy of the states with $3d_{z^2}$ and $3d_{x^2-y^2}$ hole character suggests that for systems with (small) octahedral distortions, the transition energy between these two states might be rather small. At first sight, this observation seems to give support to the suggestion made by Perkins *et al.* for a crystal-field excitation

TABLE IV. CASPT2 energies (in eV) of the *d-d* transitions in CuO for different ratios of *d* (Cu-$O_{in\text{-}plane}$) and *d* (Cu-O_{apex}).

Ratio in-plane/apex	Hole character			
	x^2-y^2	z^2	*xy*	*xz, yx*
1.00	0.00	0.00	1.02	1.02
0.95	0.00	0.28[a]	1.03	1.07
0.90	0.00	0.54[a]	1.04	1.12
0.85	0.00	0.77	1.05	1.15
0.80	0.00	0.98	1.06	1.18

[a]CASSCF wave function obtained as an average of $^2B_{1g}$ and $^2A_{1g}$, ratio 1:10.

around 0.4–0.5 eV in La_2CuO_4 and $Sr_2CuO_2Cl_2$. To further analyze this assumption, we performed a series of calculations on CuO varying the ratio between the in plane and apex Cu-O distance. Results are given in Table IV. It is obvious that for small distortions of the octahedral structure, the $^2B_{1g}\rightarrow{}^2A_{1g}$ transition has a transition energy of the order of 0.4 eV, but for larger distortions the excitation energy rapidly increases to a value of approximately 1 eV for the ratio of the two copper oxygen distances observed in La_2CuO_4. As expected, the transition in which the hole is transferred to the $3d_{xy}$ orbital—the $^2B_{1g}\rightarrow{}^2B_{2g}$ transition—does not depend on the ratio of the two distances, and the $^2B_{1g}\rightarrow{}^2E_g$ transition is only slightly dependent on this ratio. Note that the $^2B_{1g}$ and $^2A_{1g}$ state transform as the same irreducible representation in the point-group symmetry applied in the calculation, namely D_{2h} instead of the actual D_{4h} symmetry. For the smaller ratios the two states are so close in energy that in a single root optimization root flipping occurs, which prevents convergence. To avoid these problems, the $^2A_{1g}$ state has been optimized in a weighted average calculation with the $^2B_{1g}$ state. Expressing the orbitals of the $^2A_{1g}$ state in this way does not significantly influence the calculated transition energies.

The structural similarity of La_2CuO_4 and $Sr_2CuO_2Cl_2$ results in a very similar *d-d* transition spectrum for both compounds. Especially, the transitions to the $^2B_{2g}$ and ^2E_g states are very close in energy. The somewhat larger value for the transition to the $^2A_{1g}$ state in $Sr_2CuO_2Cl_2$ can be attributed to the larger Cu-L_{apex} distance in this compound. For La_2CuO_4, the excitation energies of the two higher *d-d* transitions as proposed by Falck *et al.*[11] are reproduced with reasonable accuracy. Moreover, the equivalent excitations in $Sr_2CuO_2Cl_2$ observed by Kuiper *et al.*[12] are also calculated in the correct energy region, although the $^2B_{1g}\rightarrow{}^2E_g$ transition is found somewhat lower in the calculations. However, we cannot confirm the existence of a *d-d* transition around 0.4–0.5 eV. The calculated energies of 0.99 and 1.18 eV for the lowest *d-d* transition are larger by more than 0.5 eV. The typical accuracy of the applied method is significantly better than this difference. The comparison with the model system CuO with a ratio of the two Cu-O distances similar to that found in La_2CuO_4 and $Sr_2CuO_2Cl_2$ shows that the excitation energies are very similar except for the transitions to states with $3d_{xz,yz}$ hole character. The difference for this transition is probably a consequence of the presence of the relatively large counterions.

The next compound in Table III is $CuGeO_3$. Although the coordination of the Cu ions is similar to that in $Sr_2CuO_2Cl_2$, the very different lattice structure makes the *d-d* spectrum less comparable to the previous discussed compounds. This is best illustrated by the fact that the calculation of the *d-d* transition energies for $CuGeO_3$ in a simple CuO_6 cluster embedded in point charges resembles the spectrum observed for $Sr_2CuO_2Cl_2$ quite close. Mulliken population analysis for the larger $CuO_6Ge_4Cu_2$ cluster indicates that the high formal ionic charge of Ge is reduced to a value of roughly +3 due to the formation of bonds with the oxygen anions with important covalent contributions. The results listed in Table III confirm the assignment of the peak around 1.7 eV to *d-d* transitions proposed by Bassi *et al.*[17] and Corradini *et al.*[18] The table shows that three states contribute to this peak, namely the states with $3d_{xz,yz}$ and $3d_{z^2}$ hole character and that the onset of this peak at 1.3 eV can be ascribed to the excitation of the $3d_{xy}$ state.

$YBa_2Cu_3O_6$ is the only cuprate in the series considered here with a fivefold coordination of the Cu^{2+} ions by O. The in-plane Cu-O distances are very similar to the previously considered cuprates, and hence hardly any change is observed for the $^2B_1\rightarrow{}^2B_2$ transition, which corresponds to moving the hole to the $3d_{xy}$ orbital. On the other hand, the absence of the sixth coordinating ligand influences the transition to the state with z^2 hole character ($^2B_1\rightarrow{}^2A_1$). The excitation energy increases by ~0.5 eV compared to La_2CuO_4 and $Sr_2CuO_2Cl_2$ as a consequence of the destabilizing of the $3d_{z^2}$ orbital with respect to hole occupation.

To end this section, we briefly discuss the results obtained for the spin chain compounds Ca_2CuO_3 and Sr_2CuO_3. In the first place, Table III shows that the *d-d* transition energies in both compounds are very similar, which is certainly expected given the similarity of the two crystal structures. Second, the changes in the *d-d* transitions observed for $YBa_2Cu_3O_6$ can be easily recognized. The $a^2A_g\rightarrow b^2A_g$ transition, corresponding to the transfer of the hole to the $3d_{z^2}$ orbital further increases in energy by ~0.4 eV due to lowering the copper coordination. Furthermore, it is seen from the table that the transition to the $3d_{xy}$ state occurs at a transition energy that is very comparable to the other cuprates. The small distortion of the CuO_4 squares that form the spin chains causes a small energy difference between the $^2B_{2g}$ and $^2B_{3g}$ state, which have $3d_{xz}$ and $3d_{yz}$ hole character, respectively (see also Fig. 4).

VI. CONCLUSIONS

We have performed *ab initio* cluster calculations to investigate the transition energies of the different $3d^n$ states in undoped cuprates. The combination of appropriate material models and high quality quantum chemical methods to approximate the solutions of the exact Hamiltonian of this material model allows for an accurate determination of the *d-d* transition energies in ionic TM materials. The accuracy of the method has been established for La_2NiO_4 for which unambiguous experimental data exist regarding the *d-d* transitions. As previously found for the TM oxides with a simple rocksalt structure, the calculated energies are within 0.15 eV of the experimental ones.

The results listed in Table III do not confirm the existence

of a *d-d* transition around 0.4–0.5 eV. For all cuprates studied here, the lowest *d-d* transition energy is 1 eV or higher. The difference of 0.6 eV is significantly larger than the typical accuracy of the method applied in this study. On the other hand, our calculations do confirm the interpretation of the 1.7-eV peak observed in $CuGeO_3$ as arising from *d-d* transitions. The calculated values lie in the same region and moreover, we have found indications that the shoulder at 1.3 eV also originates from a *d-d* transition.

Concerning the differences in *d-d* transitions between the compounds in the series considered here, we conclude that the transition in which the hole is transferred to the $3d_{xy}$ orbital hardly changes in energy within the whole series. The same is concluded for the transitions to the $3d_{xz}$ and $3d_{yz}$ orbitals. The only *d-d* transition that suffers large changes is the $3d_{x^2-y^2} \rightarrow 3d_{z^2}$ transition, for which the excitation energy varies from 1 eV in La_2CuO_4 to more than 2 eV in Ca_2CuO_3 and Sr_2CuO_3. These trends are directly related to the coordination of the Cu ions. The in-plane coordination is very similar in all compounds, while the coordination along the *z* axis changes from two ligands for La_2CuO_4 and $Sr_2CuO_2Cl_2$, to one ligand for $YBa_2Cu_3O_6$, to no ligand at all for Sr_2CuO_3 and Ca_2CuO_3.

ACKNOWLEDGMENTS

C.deG. acknowledges the financial support through the TMR activity ''Marie Curie research training grants'' Grant No. FMBICT983279 established by the European Community. We are very grateful to I. de P. R. Moreira and W. C. Nieuwpoort for valuable help and discussions.

*Author to whom correspondence should be addressed. Electronic address: c.degraaf@qf.ub.es

[1] Y. Mizuno and S. Koide, Phys. Kondens. Mater. **2**, 166 (1964).
[2] J. Lorenzana and G. A. Sawatzky, Phys. Rev. Lett. **74**, 1867 (1995).
[3] J. Lorenzana and G. A. Sawatzky, Phys. Rev. B **52**, 9576 (1995).
[4] J. D. Perkins, J. M. Graybeal, M. A. Kastner, R. J. Birgeneau, J. P. Falck, and M. Greven, Phys. Rev. Lett. **71**, 1621 (1993).
[5] J. D. Perkins, D. S. Kleinberg, M. A. Kastner, R. J. Birgeneau, Y. Endoh, K. Yamada, and S. Hosoya, Phys. Rev. B **52**, 9863 (1995).
[6] J. D. Perkins, R. J. Birgeneau, J. M. Graybeal, M. A. Kastner, and D. S. Kleinberg, Phys. Rev. B **58**, 9390 (1998).
[7] H. Eskes, L. H. Tjeng, and G. A. Sawatzky, Phys. Rev. B **41**, 288 (1990).
[8] R. L. Martin and P. J. Hay, J. Chem. Phys. **98**, 8680 (1993).
[9] R. Liu, D. Salamon, M. V. Klein, S. L. Cooper, W. C. Lee, S.-W. Cheong, and D. M. Ginsberg, Phys. Rev. Lett. **71**, 3709 (1993).
[10] D. Salamon, R. Liu, M. V. Klein, M. A. Karlow, S. L. Cooper, S.-W. Cheong, W. C. Lee, and D. M. Ginsberg, Phys. Rev. B **51**, 6617 (1995).
[11] J. P. Falck, J. D. Perkins, A. Levy, M. A. Kastner, J. M. Graybeal, and R. J. Birgeneau, Phys. Rev. B **49**, 6246 (1994).
[12] P. Kuiper, J.-H. Guo, C. Såthe, L.-C. Duda, J. Nordgren, J. J. M. Pothuizen, F. M. F. de Groot, and G. A. Sawatzky, Phys. Rev. Lett. **80**, 5204 (1998).
[13] M. Grüninger, J. Münzel, A. Gaymann, A. Zibold, H. P. Geserich, and T. Kopp, Europhys. Lett. **35**, 55 (1996).
[14] H. Suzuura, H. Yasuhara, A. Furusaki, N. Nagaosa, and Y. Tokura, Phys. Rev. Lett. **76**, 2579 (1996).
[15] J. Lorenzana and R. Eder, Phys. Rev. B **55**, 3358 (1997).
[16] I. Terasaki, R. Itti, N. Koshizuka, M. Hase, I. Tsukada, and K. Uchinokura, Phys. Rev. B **52**, 295 (1995).
[17] M. Bassi, P. Camagni, R. Rolli, G. Samoggia, F. Parmigiani, G. Dhalenne, and A. Revcolevschi, Phys. Rev. B **54**, 11 030 (1996).
[18] V. Corradini, A. Goldoni, F. Parmigiani, C. Kim, A. Revcolevschi, L. Sangaletti, and U. del Pennino, Surf. Sci. **420**, 142 (1999).
[19] R. Newman and R. M. Chrenko, Phys. Rev. **114**, 1507 (1959).
[20] J. B. Goodenough, in *Progress in Solid State Chemistry*, edited by H. Reiss (Pergamon Press, Oxford, 1971), p. 145.
[21] P. Odier, M. Leblanc, and J. Choisnet, Mater. Res. Bull. **21**, 787 (1986).
[22] J. D. Jorgensen, B. Dabrowski, S. Pei, D. R. Richards, and D. G. Hinks, Phys. Rev. B **40**, 2187 (1989).
[23] A. Hayashi, H. Tamura, and Y. Ueda, Physica C **216**, 77 (1993).
[24] J. M. Longo and P. M. Raccah, J. Solid State Chem. **6**, 526 (1973).
[25] L. L. Miller, X. L. Wang, S. X. Wang, C. Stassis, D. C. Johnston, J. Faber, Jr., and C.-K. Loong, Phys. Rev. B **41**, 1921 (1990).
[26] H. Völlenkle, A. Wittmann, and H. Nowotny, Monatsch. Chem. **98**, 1352 (1967).
[27] M. F. Garbauskas, R. W. Green, R. H. Arendt, and J. S. Kasper, Inorg. Chem. **27**, 871 (1988).
[28] M. Hjorth and J. Hyldtoft, Acta Chem. Scand. **44**, 516 (1990).
[29] T. Ami, M. K. Crawford, R. L. Harlow, Z. R. Wang, D. C. Johnston, Q. Huang, and R. W. Erwin, Phys. Rev. B **51**, 5994 (1995).
[30] G. J. M. Janssen and W. C. Nieuwpoort, Phys. Rev. B **38**, 3449 (1988).
[31] L. Pueyo, V. Luaña, M. Flórez, E. Francisco, J. M. Recio, and M. Bermejo, Rev. Solid State Sci. **5**, 137 (1991).
[32] M. Haßel, H. Kuhlenbeck, H. J. Freund, S. Shi, A. Freitag, V. Staemmler, S. Lütkehoff, and M. Neumann, Chem. Phys. Lett. **240**, 205 (1995).
[33] C. de Graaf, R. Broer, and W. C. Nieuwpoort, Chem. Phys. **208**, 35 (1996).
[34] A. Fujimori and F. Minami, Phys. Rev. B **30**, 957 (1984).
[35] J. van Elp, H. Eskes, P. Kuiper, and G. A. Sawatzky, Phys. Rev. B **45**, 1612 (1992).
[36] C. de Graaf, C. Sousa and R. Broer, J. Mol. Struct.: THEOCHEM **458**, 53 (1999).
[37] P.-O. Widmark, P.-Å. Malmqvist, and B. O. Roos, Theor. Chim. Acta **77**, 291 (1990).
[38] P.-O. Widmark, B. J. Persson, and B. O. Roos, Theor. Chim. Acta **79**, 419 (1991).
[39] R. Pou-Amérigo, M. Merchán, I. Nebot-Gil, P.-O. Widmark, and B. O. Roos, Theor. Chim. Acta **92**, 149 (1995).
[40] K. Andersson, P.-Å. Malmqvist, B. O. Roos, A. J. Sadlej, and K. Wolinski, J. Phys. Chem. **94**, 5483 (1990).
[41] K. Andersson, P.-Å. Malmqvist, and B. O. Roos, J. Chem. Phys. **96**, 1218 (1992).
[42] K. Andersson, M. R. A. Blomberg, M. P. Fülscher, G. Karlström, R. Lindh, P.-Å. Malmqvist, P. Neogrády, J. Olsen, B. O. Roos,

A. J. Sadlej, M. Schütz, L. Seijo, L. Serrano-Andrés, P. E. M. Siegbahn, and P.-O. Widmark, MOLCAS version 4 (University of Lund, Sweden, 1997).
[43] Z. Barandiarán and L. Seijo, Can. J. Chem. **70**, 409 (1992).
[44] H. M. Evjen, Phys. Rev. **39**, 675 (1932).
[45] R. D. Shannon, Acta Crystallogr., Sect. A: Cryst. Phys., Diffr., Theor. Gen. Crystallogr. **A32**, 751 (1976).
[46] C. de Graaf, W. A. de Jong, R. Broer, and W. C. Nieuwpoort, Chem. Phys. **237**, 59 (1998).
[47] B. O. Roos and K. Andersson, Chem. Phys. Lett. **245**, 215 (1995).